

Precise RNA targeting with CRISPR–Cas13d

Received: 13 May 2024

Accepted: 8 January 2025

Published online: 11 February 2025

 Check for updatesSydney K. Hart^{1,2}, Simon Müller^{1,2}, Hans-Hermann Wessels^{1,2},
Alejandro Méndez-Mancilla^{1,2}, Gediminas Drabavicius^{1,2}, Olivia Choi^{1,2} &
Neville E. Sanjana^{1,2} ✉

The possibility of collateral RNA degradation poses a concern for transcriptome perturbations and therapeutic applications using CRISPR–Cas13. We show that collateral activity only occurs with high *RfxCas13d* expression. Using low-copy *RfxCas13d* in transcriptome-scale and combinatorial pooled screens, we achieve high on-target knockdown without extensive collateral activity. Furthermore, analysis of a high-fidelity Cas13 variant suggests that its reduced collateral activity may be due to overall diminished nuclease capability.

Type VI CRISPR–Cas nucleases, specifically *RfxCas13d*, have been harnessed for a variety of RNA-targeting applications because of their precise and efficient knockdown of RNA transcripts^{1–3}. RNA-targeting CRISPR systems have demonstrated therapeutic potential for temporary or nonheritable edits^{2,3}; however, collateral RNA cleavage in Cas13-based RNA editing systems may limit their use for transcriptome editing in vivo. Although initial studies using *RfxCas13d* in vitro and in vivo did not detect collateral RNA degradation^{1,4,5}, recent studies have demonstrated collateral activity when highly expressed genes are targeted^{6–9}. Resolving these discrepancies requires a systematic characterization of the extent and context of collateral RNA targeting. A thorough understanding of this phenomenon and methods to mitigate it would enhance the utility of Cas13 for RNA-targeting assays, transcriptome-scale screens of coding and noncoding RNAs and the safety of future Cas13-based therapies.

One initial observation we made was that studies using transfection-based methods such as piggyBac transposons^{8,10} or liposome-mediated transfection^{6–8} of *RfxCas13d* reported higher frequencies of collateral activity than studies using viral delivery of similar constructs^{1,3–5,11–13}. Consistent with previous work suggesting that regulating *RfxCas13d* expression reduces collateral activity⁶, we hypothesized that the difference in reported collateral activity between viral and transfection-based delivery may be because of the level of *RfxCas13d* expressed. To test this, we created an *RfxCas13d*-P2A-mCherry plasmid to measure *RfxCas13d* expression by fluorescence under different delivery conditions (Fig. 1a). We transfected HEK293FT cells with different amounts of *RfxCas13d* plasmid (0, 125, 250 or 500 ng) or transduced them with a lentivirus—produced from the same plasmid—at a low multiplicity of infection (MOI). To account for DNA toxicity, we used 500 ng of total plasmid for all transfections, with inactive *RfxCas13d* plasmid compensating for any

reduction in active *RfxCas13d*-P2A-mCherry plasmid (Supplementary Fig. 1a,b). We analyzed mCherry expression using quantitative microscopy (Fig. 1b). Virally transduced cells showed similar mCherry expression to the 125 ng transfection but with more uniform expression across the population (Fig. 1b). Doubling the plasmid dose stepwise resulted in 2.4-fold and 4.4-fold higher mCherry levels in the 250-ng and 500-ng transfection conditions, respectively.

To assess whether increased *RfxCas13d* expression leads to collateral activity, we targeted the highly expressed but nonessential genes *MIF* and *B2M* (Fig. 1c and Supplementary Fig. 1c). We chose these genes because previous studies from other groups have shown that high-dose transfection of *RfxCas13d* targeting *MIF* can trigger collateral activity⁷, while targeting *B2M* in *RfxCas13d*-transduced T-cells showed no such effect³.

We added an EFS-driven *EGFP* reporter into the guide RNA (gRNA) constructs to monitor collateral activity and delivered them lentivirally into HEK293FT cells to ensure stable expression of the gRNAs and *EGFP* (Fig. 1c). Using ERCC spike-in controls to monitor any global RNA reductions caused by collateral activity, we found that transfection of higher *RfxCas13d* amounts (250 and 500 ng) led to a dose-dependent reduction in *EGFP* RNA and protein (Fig. 1d,e and Supplementary Fig. 1d,e). In contrast, lentiviral transduction at low MOI (<0.3) or lower transfection doses (125 ng) did not significantly decrease *EGFP* expression compared to controls with inactive (nuclease-null) *RfxCas13d*.

We next examined whether endogenous transcripts are similarly affected by collateral activity. Consistent with our *EGFP* results, lentiviral transduction and low-dose transfection of *RfxCas13d* did not lead to collateral degradation of endogenous transcripts (Fig. 1d,e). However, higher transfection doses caused collateral degradation and reduced cell viability, despite consistent on-target knockdown of *B2M* and *MIF* across all conditions.

¹New York Genome Center, New York, NY, USA. ²Department of Biology, New York University, New York, NY, USA. ✉e-mail: neville@sanjanalab.org

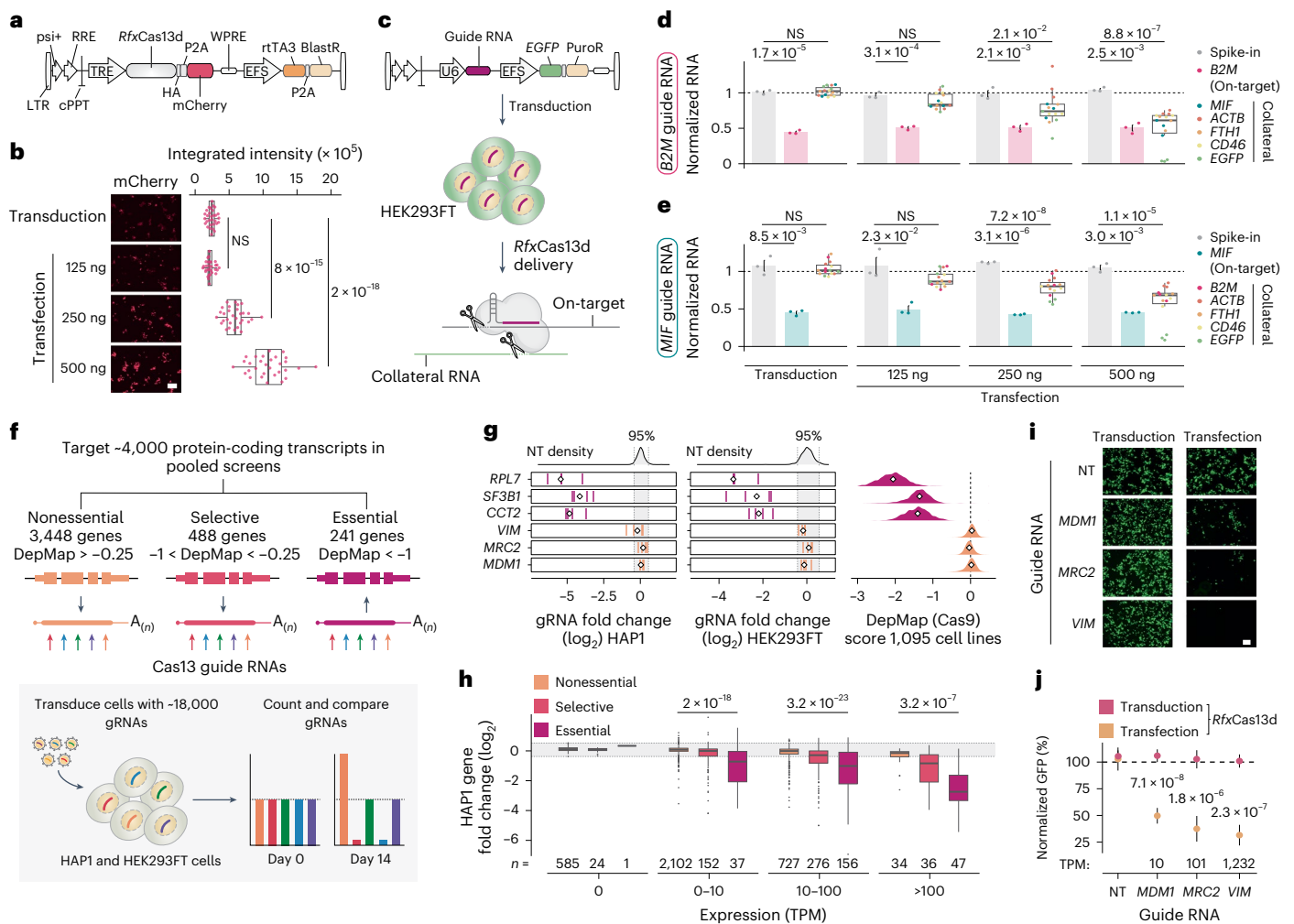


Fig. 1 | Control of *RfxCas13d* expression can mitigate collateral RNA cleavage in human cells. a, Lentiviral vector for doxycycline-inducible *RfxCas13d*-P2A-mCherry that coexpresses blasticidin resistance. **b**, Left, representative mCherry images of HEK293FT cells 4 days after being transduced or transfected with *RfxCas13d*-P2A-mCherry. Scale bar, 200 μm . Right, quantification of mCherry (*RfxCas13d*) expression across conditions ($n = 18$ images from two independent transductions or transfections). Box plots show the median and the 25th and 75th percentiles, with whiskers extending 1.5 times the interquartile range; significance was determined using a two-sided Mann–Whitney *U*-test. **c**, Lentiviral vector for Cas13 gRNAs coexpressing EGFP, transduced before *RfxCas13d*-P2A-mCherry delivery (transduced or transfected with increasing amounts), for readout of on-target knockdown and collateral RNA degradation. **d**, RNA expression for the Cas13-targeted transcript (*B2M*) and other (collateral) transcripts (*MIF*, *ACTB*, *FTH1*, *CD46* and *EGFP*) in HEK293FT stably expressing a *B2M*-targeting gRNA. RNA expression is measured using RT–qPCR relative to cells with a nuclease-inactive *RfxCas13d* as a control and normalized using ERCC spike-ins. Normalized expression is displayed as the mean \pm s.e.m. ($n = 3$ independent *RfxCas13d* transductions or transfections) with a two-tailed Student’s *t*-test. NS, not significant. **e**, RNA expression for the Cas13-targeted transcript (*MIF*) and other (collateral) transcripts (*B2M*, *ACTB*, *FTH1*, *CD46* and *EGFP*) in HEK293FT stably expressing an *MIF*-targeting gRNA. RNA expression is measured using RT–qPCR relative to cells with a nuclease-inactive *RfxCas13d* as a control and normalized using ERCC spike-ins. Normalized expression is displayed as the mean \pm s.e.m. ($n = 3$ independent *RfxCas13d* transductions or transfections) with a two-tailed Student’s *t*-test. **f**, *RfxCas13d* pooled screen with 17,708 gRNAs targeting essential and nonessential protein-coding genes (and non-targeting (NT) controls) with different transcript expression levels ($n = 4,177$ genes covering 20% of the human protein-coding transcriptome) in HEK293FT and HAP1 cells ($n = 2$ biological replicate screens per cell line).

Genes are categorized by DepMap gene essentiality: nonessential (mean DepMap score ≥ -0.25), selective ($-1 < \text{DepMap score} < -0.25$) or essential (DepMap score < -1) ($n = 1,095$ cell lines, 23Q2 release)¹⁴. After 14 days of culture, we identified whether gRNAs targeting essential, selective and nonessential genes were depleted by comparing their abundance between day 14 and day 0. **g**, Left, normalized depletion of individual gRNAs targeting essential (purple) and nonessential (yellow) genes ($n = 4$ gRNAs). The median of the gRNAs is indicated by the diamond. The distribution of the middle 95% of NT gRNAs is shown in gray. Right, the distribution of DepMap essentiality scores ($n = 1,095$ cell lines) for the indicated gene; the diamond indicates the median DepMap score. **h**, Comparison of fold change (day 14 versus day 0) from the pooled Cas13 screen and expression level of DepMap essential, selective and nonessential genes in HAP1 cells. Dashed lines indicate the distribution of the middle 95% of NT gRNAs. Box plots show the median and the 25th and 75th percentiles, with whiskers extending 1.5 times the interquartile range. Statistical significance was determined using a two-sided Mann–Whitney *U*-test. **i**, Representative images of human HEK293FT cells transduced with NT, *MDM1*-targeting, *MRC2*-targeting or *VIM*-targeting gRNAs and subsequent transfection of a GFP reporter vector for collateral readout. *MDM1*, *MRC2* and *VIM* are nonessential genes (**g**). Cells were either transduced or transfected with *RfxCas13d*. Scale bar, 100 μm . **j**, GFP expression in HEK293FT cells after transduction with NT, *MDM1*-targeting, *MRC2*-targeting or *VIM*-targeting gRNAs and subsequent transfection of a GFP reporter vector. Before gRNA and GFP reporter delivery, cells were either transduced or transfected (250 ng) with active or catalytically inactive *RfxCas13d*. GFP expression was normalized to inactive *RfxCas13d*-expressing cells (transduced or transfected, as indicated). Error bars indicate the mean \pm s.d. and significance was determined using a two-sided *t*-test ($n = 2$ gRNAs per gene, with three biological replicates per gRNA).

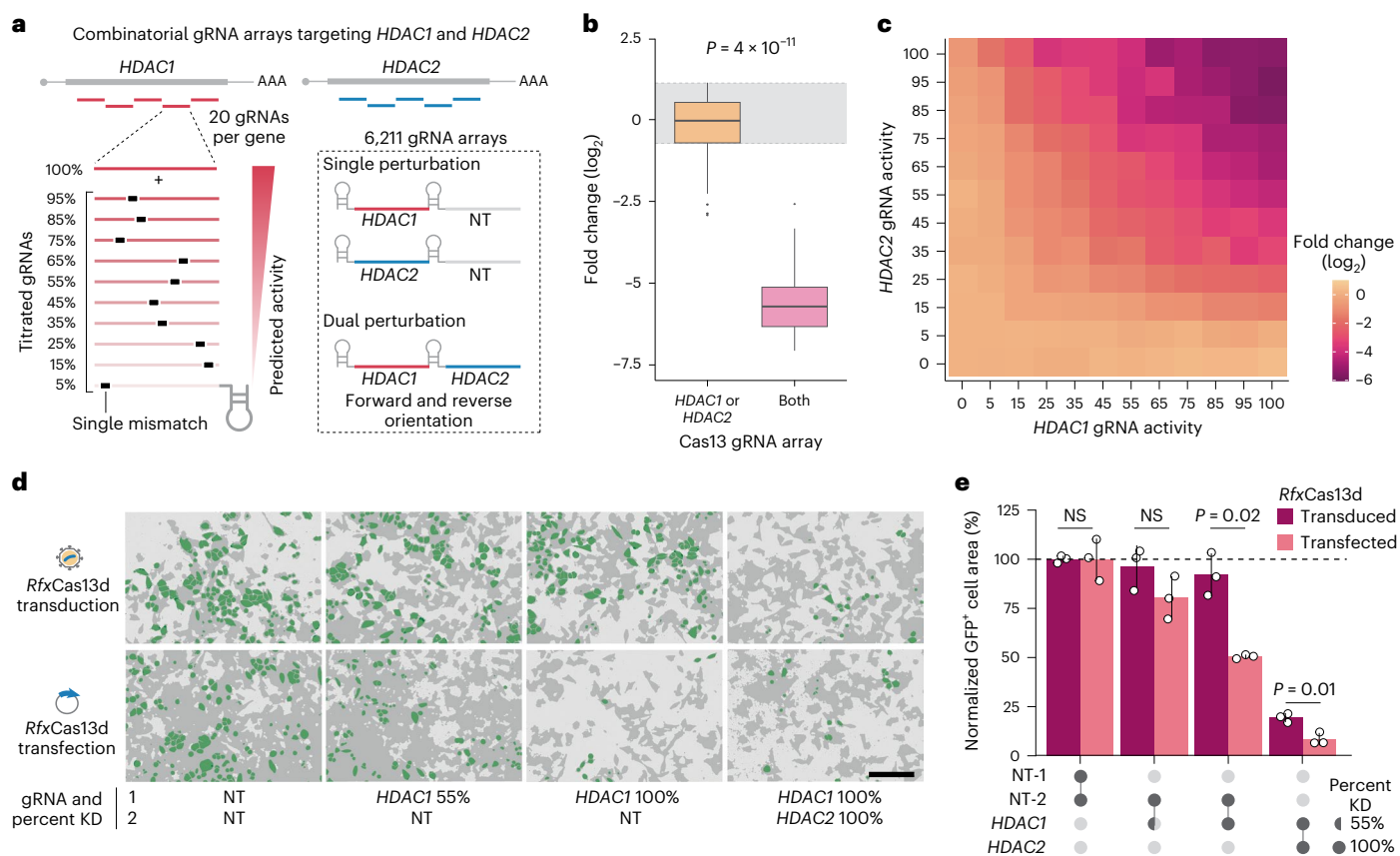


Fig. 2 | Combinatorial knockdown of synthetic lethal gene pair *HDAC1*–*HDAC2* confirms lack of collateral RNA cleavage after low-copy-number transduction of *RfxCas13d*. **a**, A combinatorial titration pooled transcriptomic screen targeting a synthetic lethal gene pair (*HDAC1* and *HDAC2*). Designed position-specific mismatches in the gRNA arrays titrate knockdown activity of *RfxCas13d*. After gRNA library transduction into human A375 cells, depletion of gRNAs containing single or dual gene perturbations is quantified by comparing gRNA counts between day 14 and day 0. **b**, Fold change of gRNAs targeting *HDAC1* or *HDAC2* individually or together at 100% predicted gRNA activity 14 days after *RfxCas13d* induction ($n = 120$ gRNA arrays with 40 each for *HDAC1* only, *HDAC2* only and both *HDAC1* and *HDAC2* targeting). The distribution of the central 95% of non-targeting (NT) control gRNAs is shown in gray ($n = 492$ NT perturbations). Box plots show the median and the 25th and 75th percentiles, with whiskers extending 1.5 times the interquartile range. Statistical significance was determined by a two-sided Mann–Whitney *U*-test. **c**, Median fold change of

dual gRNA perturbations (targeting *HDAC1* and *HDAC2*), binned on the basis of predicted gRNA activity ($n = 40$ gRNA arrays per gene-targeting heat map tile; $n = 492$ gRNA arrays for NT perturbations (0×0 heat map tile)). **d**, Representative images of a competition assay using A375 cells transduced with dual gRNA arrays targeting *HDAC1* and *HDAC2* at 55% or 100% predicted gRNA activity or NT gRNAs and imaged 5 days later. The dual gRNA array constructs also constitutively express GFP; these cells were mixed 1:1 with cells without a dual gRNA array (nonfluorescent cells) at the time of plating. Cells with and without GFP or array were either transduced or transfected (250 ng) with *RfxCas13d* as indicated. Scale bar, 200 μm . **e**, Percentage of GFP-positive cells for each gRNA array normalized to NT gRNA array control for both transduced and transfected (250 ng) *RfxCas13d* cells ($n = 27$ images from three independent transductions or transfections; mean \pm s.d.). Statistical significance was determined with a two-sided *t*-test.

Because we observed no collateral activity on both exogenous and native transcripts when targeting *MIF* and *B2M* by viral transduction, we sought to assess this more comprehensively across the transcriptome. Using pooled Cas13 screens in two human cell lines (HAP1 and HEK293FT), we targeted approximately 20% of all protein-coding genes—spanning a wide range of expression levels—with multiple gRNAs per gene (Fig. 1f, Supplementary Fig. 2a and Supplementary Table 1). In total, we targeted 3,448 nonessential genes, as classified by DepMap¹⁴, with four gRNAs each to comprehensively assess collateral degradation. We also included 241 essential genes and 488 selective (moderately essential) genes to monitor their depletion as positive controls. Prior studies have linked *RfxCas13d* collateral activity to reduced cell viability because of RNase-like chromatin collapse and 28S ribosomal RNA cleavage⁷⁹. Thus, if collateral activity occurred in our screens, we would expect to see depletion of highly expressed nonessential genes because of unintended transcript degradation.

In line with our prior experiments targeting *MIF* and *B2M*, we found that gRNAs targeting nonessential genes did not deplete in the pooled

screens regardless of the target gene’s expression levels (Fig. 1g,h, Supplementary Fig. 2b,c and Supplementary Table 2). In contrast, gRNAs targeting essential genes readily depleted, demonstrating that on-target knockdown is highly efficient. As expected, gRNAs targeting genes classified as selective in DepMap also depleted but not to the same degree as those classified as essential. Subsequently, we individually targeted three nonessential genes from this screen with low (*MDMI*, 10 transcripts per million reads (TPM)), medium (*MRC2*, 101 TPM) or high (*VIM*, 1232 TPM) expression in HEK293FT cells that were either transduced with *RfxCas13d* lentivirus or transfected with the same vector. Using cotransfected GFP as a readout for collateral activity, we found that only transfection of *RfxCas13d* results in collateral GFP degradation and that GFP depletion positively correlates with the targeted gene’s expression (Fig. 1i,j).

Next, we investigated whether modifying the gRNA sequence could diminish the recognition of the target RNA transcript and hinder the conformational changes necessary for *cis* and *trans* RNA cleavage. We performed a combinatorial *RfxCas13d* screen in A375 cells

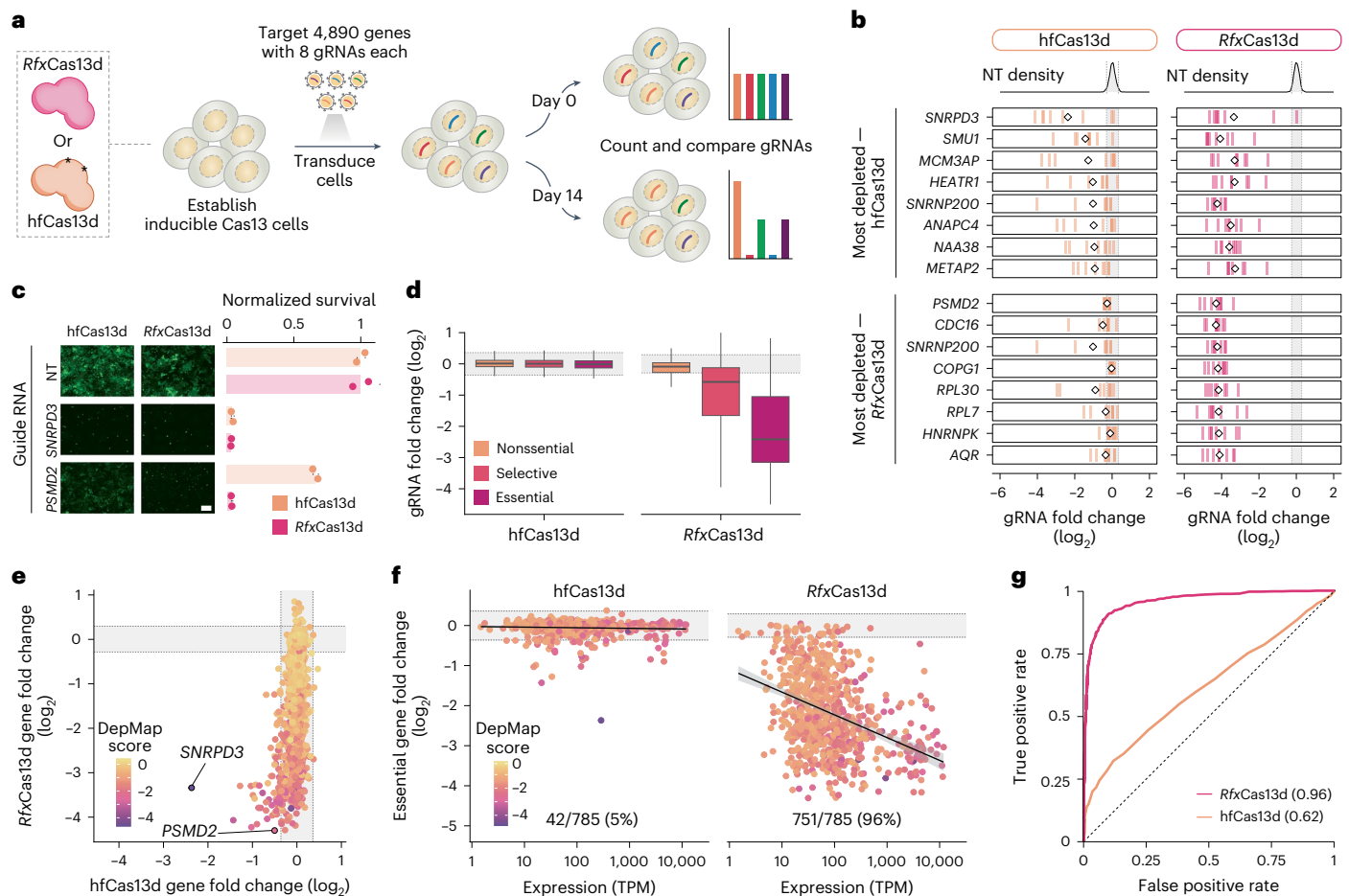


Fig. 3 | A high-fidelity Cas13d variant (hfCas13d) that minimizes collateral RNA cleavage has substantially less on-target knockdown. **a**, The *RfxCas13d* and *hfCas13d* screens compare nuclease-specific differences in gene depletion for low-copy-number transduction. After library transduction into HAP1 cells, gRNA depletion is quantified by comparing gRNA counts between day 14 and day 0. **b**, Depletion of gRNAs (day 14 versus day 0) targeting the top eight most depleted genes from the *hfCas13d* (orange) and *RfxCas13d* (blue) screens ($n = 8$ gRNAs per gene). The mean of the eight gRNAs is indicated by the diamond. **c**, Left, representative images of *hfCas13d* and *RfxCas13d* HAP1 cells transduced with individual gRNAs targeting *SNRPD3* or *PSMD2* relative to those transduced with a NT gRNA. Right, survival of GFP-positive cells containing *SNRPD3*-targeting or *PSMD2*-targeting gRNAs were normalized to the non-targeting (NT) control gRNA ($n = 2$ replicates per perturbation). **d**, For the indicated Cas13 nuclease, the fold change of gRNAs (day 14 versus day 0) is shown, categorized by DepMap gene

essentiality: nonessential (mean DepMap score ≥ -0.25), selective ($-1 < \text{DepMap score} < -0.25$) or essential (DepMap score < -1) ($n = 1,095$ cell lines). Box plots show the median and the 25th and 75th percentiles, with whiskers extending 1.5 times the interquartile range. **e**, Fold change of all genes in the *RfxCas13d* and *hfCas13d* screens ($n = 4,890$ genes). The color denotes gene essentiality (mean DepMap score). **f**, Depletion of essential genes (mean DepMap score < -1) as a function of target gene expression genes ($n = 785$ highly essential genes). Each gene is colored by its mean DepMap score. The percentage of genes depleted is quantified on the basis of whether a gene is more depleted than the 99th percentile of the NT gRNA distribution. **g**, ROC curve for DepMap essential genes compared to nonessential genes ($n = 785$ essential genes, $n = 1,985$ nonessential genes). Numbers in parentheses next to each Cas13 protein indicate the AUROC. For panels **b**, **e** and **f**, the distribution of the central 98% of the NT gRNAs are shown in grey.

targeting *HDAC1* and/or *HDAC2* using $\sim 6,000$ pairs of gRNAs. These two genes formed a synthetic lethal gene pair, where targeting both genes (but not either singly) resulted in lethality and dropout, as shown in a recent study using DNA-targeting perturbations¹⁵ (Supplementary Fig. 3a). We took advantage of our TIGER (targeted inhibition of gene expression through gRNA design) model¹³ to design titrated gRNAs with single mismatches in the parent sequence that alter the expected transcript knockdown activity over a range of partial knockdowns (Fig. 2a, Supplementary Fig. 3b and Supplementary Table 3). Targeting a single gene from the pair should decrease cell fitness because of the high expression levels of these genes—147 TPM for *HDAC1* and 130 TPM for *HDAC2*—if unintended collateral activity occurs.

In line with our previous findings, targeting either *HDAC1* or *HDAC2* alone from the synthetic lethal pair did not result in significant gRNA depletion in low-copy *RfxCas13d* cell lines (Fig. 2b, Supplementary Fig. 3c and Supplementary Fig. 4a,b). As expected,

targeting both genes in the same cell led to gRNA depletion. The level of depletion across all titration pairs correlated with the predicted activity of the partial knockdown gRNAs (Fig. 2c and Supplementary Fig. 4a–d).

To understand how mismatches in the gRNA sequence affect knockdown efficiency, we performed RNA immunoprecipitation (RIP) in A375 cells expressing inactive *RfxCas13d* and *HDAC1*-targeting gRNAs, with and without mismatches (Supplementary Fig. 5a). We confirmed that reduced knockdown activity for mismatched gRNAs was because of weaker binding to the target transcript (Supplementary Fig. 5b,c), consistent with the observed knockdown of *HDAC1* at both RNA and protein levels (Supplementary Fig. 5d,e).

To confirm that the lack of collateral activity in this screen was a result of the low copy number of *RfxCas13d*, we performed a competition assay and targeted *HDAC1* and/or *HDAC2* using either transfected or transduced *RfxCas13d* (Fig. 2d,e). As before, we observed

depletion when both *HDAC1* and *HDAC2* were targeted, regardless of how *RfxCas13d* was delivered. However, when targeting *HDAC1* alone, we only observed depletion of cells when *RfxCas13d* was delivered by transfection. Notably, targeting *HDAC1* using perfect-match gRNAs resulted in a significant decrease in GFP in the transfection condition. Even with imperfect match gRNAs (predicted knockdown of 55%), we observed a slight decrease in GFP signal in the transfection condition. This confirms that modulating the rate of target recognition with designed mismatches in the gRNA alters not only *cis* RNA cleavage but also *trans* collateral cleavage.

With growing interest in high-fidelity variants of *RfxCas13d* for transcriptome engineering^{16,17}, we evaluated the activity of a recently described variant (hfCas13d)⁸. We generated a doxycycline-inducible hfCas13d HAP1 cell line by lentiviral transduction at low MOI and tested on-target knockdown with gRNAs targeting *CD46* and *CD55* (Supplementary Fig. 6a–c). We found that hfCas13d has a ~4-fold weaker knockdown efficiency compared to *RfxCas13d*, despite similar nuclease expression. To compare their activities on a larger scale, we performed a pooled screen targeting 4,890 genes with eight gRNAs each¹³ (Fig. 3a, Supplementary Fig. 6d and Supplementary Table 4). We found that the top eight most depleted genes from the hfCas13d screen showed weaker gRNA depletion and greater variability compared to *RfxCas13d* (Fig. 3b). We confirmed these results by individually targeting the most depleted gene from each screen (*PSMD2* for the *RfxCas13d* screen, *SNRPD3* for the hfCas13d screen). Only in *RfxCas13d*-expressing cells did we observe strong depletion when targeting both of these genes (Fig. 3c).

Notably, while some gRNAs did deplete from the hfCas13d screen, the vast majority of genes, even those that were selective or essential, did not—a stark contrast to *RfxCas13d* (Fig. 3d and Supplementary Fig. 6e,f). When comparing *RfxCas13d* and hfCas13d screens on a gene level, we found that 1,455 genes had a twofold or greater depletion in the *RfxCas13d* screen, whereas only five of the 4,890 genes had a twofold or greater depletion in the hfCas13d screen (Fig. 3e, Supplementary Table 5). For high-confidence essential genes, we found that 96% of targeted genes depleted in the *RfxCas13d* screen but only 5% depleted in the hfCas13d screen (DepMap Chronos essentiality score ≤ -1 ; $n = 785$ genes) (Fig. 3f). Importantly, we successfully discriminated essential genes from nonessential genes with *RfxCas13d* (area under the receiver operating characteristic curve (AUROC) = 0.96) but not with hfCas13d (AUROC = 0.62) because of a lack of depletion among gRNAs targeting essential genes (Fig. 3g).

To investigate whether reduced gRNA depletion in the hfCas13d screen stemmed from differences in target binding and/or cleavage, we used HAP1 cell lines expressing either inactive or active *RfxCas13d* and hfCas13d while targeting *SNRPD3* and *PSMD2*. We compared RNA binding by RIP in the inactive *RfxCas13d*/hfCas13d cell lines and RNA cleavage using qPCR in the active *RfxCas13d*/hfCas13d cell lines. RIP revealed that *RfxCas13d* had 3.3-fold and 13.1-fold higher transcript-binding enrichment for *SNRPD3* and *PSMD2*, respectively, compared to hfCas13d (Supplementary Fig. 7a–d). While *SNRPD3* knockdown was similar for both variants (90% for hfCas13d, 94% for *RfxCas13d*), *PSMD2* knockdown was significantly weaker with hfCas13d (28% versus 83%), which aligned with its lower transcript binding and milder phenotypic effect (Fig. 3c and Supplementary Fig. 7e,f). These findings suggest that the mutations in hfCas13d alter gRNA preferences and reduce its binding efficiency, leading to lower gRNA depletion in functional transcriptomic screens. Optimized gRNA designs may improve hfCas13d's performance but its current limitations make it less suitable for high-efficiency knockdown in large-scale screens.

Overall, our results highlight the importance of regulating *RfxCas13d* expression to avoid collateral RNA degradation. Using low-copy lentiviral transduction, *RfxCas13d* achieved robust on-target knockdown without collateral effects. Although high-fidelity Cas13 variants can reduce collateral activity, they do so at the cost of knockdown

efficiency. As transcriptome engineering and Cas13-based functional screens advance, careful selection of Cas13 variants and delivery methods is crucial to balancing high on-target activity with minimal collateral RNA degradation.

Online content

Any methods, additional references, Nature Portfolio reporting summaries, source data, extended data, supplementary information, acknowledgements, peer review information; details of author contributions and competing interests; and statements of data and code availability are available at <https://doi.org/10.1038/s41587-025-02558-3>.

References

- Konermann, S. et al. Transcriptome engineering with RNA-targeting type VI-D CRISPR effectors. *Cell* **173**, 665–676 (2018).
- Zhang, F. et al. Multiplexed inhibition of immunosuppressive genes with Cas13d for combinatorial cancer immunotherapy. *Nat. Biotechnol.* <https://doi.org/10.1038/s41587-024-02535-2> (2025).
- Tieu, V. et al. A versatile CRISPR–Cas13d platform for multiplexed transcriptomic regulation and metabolic engineering in primary human T cells. *Cell* **187**, 1278–1295 (2024).
- Wessels, H.-H. et al. Massively parallel Cas13 screens reveal principles for guide RNA design. *Nat. Biotechnol.* **38**, 722–727 (2020).
- Morelli, K. H. et al. An RNA-targeting CRISPR–Cas13d system alleviates disease-related phenotypes in Huntington's disease models. *Nat. Neurosci.* **26**, 27–38 (2023).
- Kelley, C. P., Haerle, M. C. & Wang, E. T. Negative autoregulation mitigates collateral RNase activity of repeat-targeting CRISPR–Cas13d in mammalian cells. *Cell Rep.* **40**, 11226 (2022).
- Shi, P. et al. Collateral activity of the CRISPR/*RfxCas13d* system in human cells. *Commun. Biol.* **6**, 1–8 (2023).
- Tong, H. et al. High-fidelity Cas13 variants for targeted RNA degradation with minimal collateral effects. *Nat. Biotechnol.* **41**, 108–119 (2023).
- Li, Y. et al. The collateral activity of *RfxCas13d* can induce lethality in a *RfxCas13d* knock-in mouse model. *Genome Biol.* **24**, 20 (2023).
- Wei, J. et al. Deep learning and CRISPR–Cas13d ortholog discovery for optimized RNA targeting. *Cell Syst.* **14**, 1087–1102 (2023).
- Guo, X. et al. Transcriptome-wide Cas13 guide RNA design for model organisms and viral RNA pathogens. *Cell Genom.* **1**, 100001 (2021).
- Wessels, H.-H. et al. Efficient combinatorial targeting of RNA transcripts in single cells with Cas13 RNA Perturb-seq. *Nat. Methods* **20**, 86–94 (2023).
- Wessels, H.-H. et al. Prediction of on-target and off-target activity of CRISPR–Cas13d guide RNAs using deep learning. *Nat. Biotechnol.* **42**, 628–637 (2024).
- Hart, T. et al. High-resolution CRISPR screens reveal fitness genes and genotype-specific cancer liabilities. *Cell* **163**, 1515–1526 (2015).
- DeWeirdt, P. C. et al. Optimization of AsCas12a for combinatorial genetic screens in human cells. *Nat. Biotechnol.* **39**, 94–104 (2021).
- Zhao, F. et al. A strategy for Cas13 miniaturization based on the structure and AlphaFold. *Nat. Commun.* **14**, 5545 (2023).
- McCallister, T. X. et al. A high-fidelity CRISPR–Cas13 system improves abnormalities associated with C9ORF72-linked ALS/FTD. *Nat. Commun.* **16**, 460 (2025).

Publisher's note Springer Nature remains neutral with regard to jurisdictional claims in published maps and institutional affiliations.

Springer Nature or its licensor (e.g. a society or other partner) holds exclusive rights to this article under a publishing agreement with the author(s) or other rightsholder(s); author

self-archiving of the accepted manuscript version of this article is solely governed by the terms of such publishing agreement and applicable law.

© The Author(s), under exclusive licence to Springer Nature America, Inc. 2025

Methods

Plasmid design and cloning

Cas13 expression plasmids were cloned using Gibson assembly (New England Biolabs (NEB), E2611L) with inserts amplified with appropriate overhangs using Q5 high-fidelity DNA polymerase (NEB, M0491L). To construct pLentiRNACRISPR_010 (Addgene, 228555), we added a P2A-mCherry cassette to *RfxCas13d* in pLentiRNACRISPR_007 (Addgene, 138149). For the comparisons with hfCas13d, we modified pLentiRNACRISPR_007 and replaced *RfxCas13d* with hfCas13d N2V8 (ref. 8) (a modified form of *RfxCas13d* with the following point substitutions: A134V, A140V, A141V and A143V). We termed this plasmid pLentiRNACRISPR_008 (Addgene, 223173). For all experiments using catalytically inactive Cas13 variants (R239A;H244A;R858A;H863A), we cloned inactive variants of *RfxCas13d* (pLentiRNACRISPR_011; Addgene, 228557) and hfCas13d (pLentiRNACRISPR_012; Addgene, 228558) into the pLentiRNACRISPR_007 backbone. For cell viability and collateral activity assays with GFP readout, we exchanged the puromycin resistance cassette in pLentiRNAGuide_001 (Addgene, 138150) with an EGFP-P2A-Puro cassette from pLentiRNAGuide_003 (Addgene, 192505) using NheI and ApaI restriction sites. We termed this new vector pLentiRNAGuide_004 (Addgene, 223175). We cloned individual gRNAs or gRNA arrays into this plasmid using Esp3I sites and T7 ligation. All plasmids were confirmed by Sanger and/or nanopore sequencing (Azenta and Plasmidsaurus). All individual guide sequences cloned in pLentiRNAGuide_003 or pLentiRNAGuide_004 are listed in Supplementary Table 6.

Cell culture and lentiviral transduction of Cas13 variants

HEK293FT (Thermo Fisher Scientific, R70007), A375 (American Type Culture Collection (ATCC), CRL-1619) and MDA-MB-231 (ATCC, HTB-26) cells were cultured in D10 medium, which is DMEM with high glucose and stabilized L-glutamine (Caisson, DML23) supplemented with 10% FBS (Sigma, I4009C). HAP1 (Horizon, C631) cells were cultured in I10 medium, which is Iscove's modified Dulbecco's medium with L-glutamine (Caisson, IML02) supplemented with 10% FBS. All cells were incubated at 37 °C with 5% carbon dioxide.

Lentivirus was produced by transfection of plasmids expressing Cas13 variants with lentiviral packaging plasmids using linear polyethylenimine (PEI) (molecular weight (MW) = 25,000; Polysciences, 23966) in HEK293FT. Cells were seeded at 10 million per well in a 10-cm plate and transfected with 75 µl of PEI, 15 µg of lentiviral Cas13 transfer plasmid (pLentiRNACRISPR_007/008/010/011/012), 12.5 µg of psPAX2 (Addgene, 12260) and 5 µg of pMD2.G (Addgene, 12259). Then, 2 days after transfection, the viral supernatant was collected and filtered through a 0.45-µm filter and then stored at -80 °C until further use.

Monoclonal doxycycline-inducible hfCas13d HAP1 cells were generated by transducing cells with an hfCas13d-expressing lentivirus at a low MOI (<0.1) and selected with 5 µg ml⁻¹ blasticidin S (AG Scientific, B-1247). Single-cell colonies were isolated by low-density plating and then expression of HA-tagged hfCas13d was confirmed by immunoblot using an anti-HA peptide antibody (Cell Signaling Technology, 2367S). hfCas13d knockdown activity was confirmed by flow cytometry using APC anti-CD46 and FITC anti-CD55 (BioLegend, 352405 and 311306, respectively). Monoclonal doxycycline-inducible *RfxCas13d*-NLS HEK293FT, A375 and HAP1 cells were previously validated by Wessels and Méndez-Mancilla et al.⁴ and Guo et al.¹¹. All monoclonal cell lines with Cas13 (or variants) were cultured with 5 µg ml⁻¹ blasticidin S. Doxycycline-inducible nuclease-active or inactive Cas13 variant-expressing cells (HEK293FT, A375 or HAP1) were generated by transducing cells with the respective lentivirus (encoding nuclease-active *RfxCas13d*-P2A-mCherry, inactive *RfxCas13d* or hfCas13d) at a low MOI and selected with 5 µg ml⁻¹ blasticidin S.

Plasmid transfection of *RfxCas13d*

We performed plasmid transfections using Lipofectamine 3000 (Thermo Fisher Scientific, L3000008). For Fig. 1b–e, HEK293FT cells were seeded at a density of 5 × 10⁵ cells per well in a 12-well plate, with 500 ng of total plasmid DNA transfected per well. To titrate the Cas13 expression, we used 0, 125, 250 and 500 ng of active *RfxCas13d* plasmid, adjusting the total to 500 ng by adding catalytically inactive *RfxCas13d* plasmid. For each well, the appropriate amount of either active *RfxCas13d* (pLentiRNACRISPR_010) or inactive *RfxCas13d* (pLentiRNACRISPR_011) plasmid, based on the titration, was first added to 50 µl of Opti-MEM I reduced-serum medium (Gibco, 31985062), containing 2 µl of P3000 reagent. Separately, 3 µl of Lipofectamine 3000 reagent was mixed with 50 µl of prewarmed Opti-MEM and this Lipofectamine mixture was then added to the DNA mixture. After a 10-min incubation, the combined mixture was added dropwise to the cells.

For Fig. 1i,j, HEK293FT cells (2 × 10⁵ per well in a 12-well plate) were seeded and cotransfected the next day with 50 ng of pmaxGFP (Lonza) and 250 ng of *RfxCas13d* (pLentiRNACRISPR_007) or inactive *RfxCas13d* (pLentiRNACRISPR_011) plasmid for the collateral cleavage readout. For experiments in Fig. 2d,e, A375 cells (2.5 × 10⁵ per well in a 12-well plate) were transfected with 250 ng of *RfxCas13d* (pLentiRNACRISPR_007). In all cases, the transfection protocol was the same as for Fig. 1b–e. Of relevance to the transfection experiments, the Cas13 (lentiviral) plasmids contained a cytomegalovirus promoter before the 5' long terminal repeat.

Lentiviral production and transduction of gRNA vectors

Lentivirus was produced by transfection of plasmids expressing *RfxCas13d* gRNAs under the U6 promoter with lentiviral packaging plasmids using linear PEI (MW = 25,000; Polysciences, 23966) in HEK293FT. Cells were seeded at 1 million per well in a six-well plate and transfected with 7.5 µl of PEI, 1.2 µg of lentiviral gRNA transfer plasmid (pLentiRNAGuide_003/004), 0.825 µg of psPAX2 (Addgene, 12260) and 0.55 µg of pMD2.G (Addgene, 12259). Then, 2 days after transfection, the viral supernatant was collected and filtered through a 0.45-µm filter and then stored at -80 °C until further use.

For transductions of single or dual gRNAs, 200 µl of lentivirus was added to 250,000 cells of the appropriate cell line along with 8 µg ml⁻¹ polybrene (Santa Cruz Biotechnology, sc-134220). The media was changed 24 h after transduction with 1 µg ml⁻¹ puromycin (Thermo Fisher Scientific, A1113803) added. Puromycin selection was completed within 48 h for all cell lines, as determined by complete killing of untransduced control cells in puromycin medium.

Western blot

Transduced A375 or HAP1 cells were collected 48 h after doxycycline induction (Sigma, D3447; 1 µg ml⁻¹), washed with 1× Dulbecco's PBS (DPBS, Sigma D8537) and lysed with total lysis buffer (50 mM Tris pH 7.4; Thermo Fisher Scientific, 15567027), 50 mM NaCl (Sigma, S5150), 2 mM MgCl₂ (Sigma, M1028) and 1% SDS (Sigma, L3771) supplemented with benzonase (MilliporeSigma, 70746-4; 0.5 µl per 100 µl of lysis buffer) for 15 min at room temperature. The protein concentration was determined using the BCA protein assay (Thermo Fisher Scientific, 23227). Equal amounts of cell lysates (20 µg) were denatured in NuPAGE LDS sample buffer (Thermo Fisher Scientific, P0007) supplemented with 100 mM DTT (Cayman, 700416) for 10 min at 65 °C. Denatured samples and PageRuler prestained protein ladder (Thermo Fisher Scientific, 26616) were separated in Novex 4–12% Tris-glycine mini gels (Thermo Fisher Scientific, XPO4125) in 1× Tris-glycine-SDS buffer (IBI Scientific, IBI01160) for 1 h at 180 V. Proteins were transferred on a nitrocellulose membrane (BioRad, 1620112) in 1× Tris-glycine transfer buffer (Thermo Fisher Scientific, LC3675) supplemented with 10% methanol for 1 h at 30 V. Immunoblots were blocked for 60 min in 5% BSA (VWR, AAJ65097) dissolved in 1× Tris-buffered saline with 1% Tween-20 (TBS-T). The membranes were then incubated overnight at 4 °C with

the following primary antibodies: anti-HA (Cell Signaling Technology, 2367S), anti-HDAC1 (Proteintech, 10197-1-AP) or anti- β -tubulin (Invitrogen, 32-2600). All primary antibodies were used at a 1:2,000 dilution in 5% BSA/TBS-T. After primary antibody incubation, the immunoblots were incubated with IRDye 800CW donkey anti-mouse secondary antibody (LI-COR, 925-32212; 1:10,000 dilution in 5% BSA/TBS-T) for 60 min at room temperature. The blots were visualized using an Odyssey CLx imaging system (LI-COR).

Flow cytometry

For flow cytometry analysis, 2×10^5 cells per condition were stained with anti-CD46 and anti-CD55 antibody (anti-CD46: BioLegend, 352405, clone TRA-2-10, 0.7 μ l per 2×10^5 cells; anti-CD55: BioLegend 311306, clone JS11, 1 μ l per 2×10^5 cells). Cells were gated by forward and side scatter and signal intensity to remove potential multiplets and additionally gated for living cells using DAPI exclusion (Thermo Fisher Scientific, L34963). For each sample, we analyzed at least 5,000 cells using FlowJo software (version 10.10.0). If cell numbers varied, we downsampled all conditions to the same number of cells before calculating the mean fluorescence intensity.

Quantitative microscopy

To measure *RfxCas13d* expression using mCherry quantification, HEK293FT cells transfected with different amounts of active *RfxCas13d*-P2A-mCherry and inactive *RfxCas13d* plasmids were compared to HEK293FT cells transfected with *RfxCas13d*-P2A-mCherry lentivirus. Images were taken using an Incucyte S3 (Sartorius) at $\times 20$ magnification at 4 days after doxycycline induction ($1 \mu\text{g ml}^{-1}$). The mCherry fluorescence intensity was calculated from nine images per condition by determining the red calibrated units in μm^2 per image (surface fit segmentation with default parameters, Incucyte live-cell analysis).

To compare collateral activity on the EGFP reporter and cell proliferation, we transduced HEK293FT-*RfxCas13d*-P2A-mCherry and HEK293FT-inactive-*RfxCas13d* with lentivirus containing *MIF* or *B2M* gRNAs (in pLentiRNAguide_004 vector) and selected with $1 \mu\text{g ml}^{-1}$ puromycin for 48 h. In parallel, HEK293FT wild-type cells were transduced with the same gRNAs and selected using $1 \mu\text{g ml}^{-1}$ puromycin for 48 h. Then, gRNA-expressing HEK293FT cells were transfected with differing amounts of active *RfxCas13d*-P2A-mCherry and inactive *RfxCas13d* plasmids. Images were taken from each well using an Incucyte S3 at $\times 20$ magnification at 4 days after doxycycline induction ($1 \mu\text{g ml}^{-1}$). The median GFP fluorescence intensity was calculated from nine images per replicate by determining the green calibrated units in μm^2 per image (surface fit segmentation with default parameters, Incucyte live-cell analysis). The median cell confluence per replicate was determined from nine images per well on phase-contrast images (artificial intelligence confluence segmentation, Incucyte live-cell analysis). For each replicate, the normalized GFP intensities were calculated by dividing the fluorescence intensity per replicate (median over nine images) for cells with active *RfxCas13d*-P2A-mCherry by those with inactive *RfxCas13d*. The normalized cell areas were calculated by dividing the confluence area per replicate (median over nine images) for cells with active *RfxCas13d*-P2A-mCherry by those with inactive *RfxCas13d*. In each case, we normalized transduced or transfected active *RfxCas13d* with inactive *RfxCas13d* with matched delivery (transduction or transfection).

For screen 1 validation, cotransfected GFP was imaged using a BZ-X Filter FITC (Keyence, OP-87764) on a BZ-X810 microscope (Keyence). Images were taken at $10\times$ magnification. For quantification, 12 representative images were taken in each well and the mean fluorescence intensity (per image) was averaged across all images to generate a mean fluorescence intensity per replicate (BZ-H4C/Hybrid Cell Count software).

Competition assays for cell growth and live imaging

For competition assays, we transduced A375-*RfxCas13d* or A375 wild-type cells with lentivirus containing dual array gRNAs in pLentiRNAguide_004 vector. We performed independent transductions for each gRNA array in triplicate and selected cells with $1 \mu\text{g ml}^{-1}$ puromycin for 3 days. The GFP-positive cells were cocultured with parental cells in equal ratios for 24 h and the ratio of GFP-positive to total cells was determined using an Incucyte S3 (Sartorius) at $\times 20$ magnification. Cas13 expression was then induced with $1 \mu\text{g ml}^{-1}$ doxycycline and the GFP-positive/GFP-negative cell ratio was observed over the course of 5–7 days with nine images per well being taken at 8-h intervals. Survival of perturbed cells was calculated by normalizing ratios to the initial time point before Cas13 induction per well and comparing to the median of cell mixtures containing cells that were transduced with nontargeting (NT) gRNA arrays. Representative images show confluence masks of GFP-positive and GFP-negative cells.

For live-cell imaging to compare *RfxCas13d* and *hfCas13d*, we transduced *RfxCas13d*-expressing or *hfCas13d*-expressing HAP1 cells with lentivirus containing gRNAs in pLentiRNAguide_004 vector, which also expresses EGFP. We performed independent transductions for each gRNA in duplicate and selected cells with $1 \mu\text{g ml}^{-1}$ puromycin for 3 days. The GFP mean fluorescence intensity was averaged across all images at $\times 20$ magnification to generate the mean fluorescence intensity per well over the course of 4 days following the induction of *RfxCas13d* and *hfCas13d* expression ($1 \mu\text{g ml}^{-1}$ doxycycline). Each well was first normalized by the intensity of the initial time point after Cas13d transfection. Loss of GFP-expressing cells was calculated by dividing the mean fluorescence intensity per well for cells transduced with targeting gRNAs by those transduced with NT gRNAs. All gRNA sequences for these validations are given in Supplementary Table 6.

Reverse transcription (RT)-qPCR

Total RNA was isolated using the Direct-zol RNA purification kit (Zymo, R2062) with DNaseI treatment. For RT-qPCR in Fig. 1, 500 ng of total RNA and 1 μ l of ERCC RNA spike-in mix (Thermo Fisher Scientific, 4456740; 1:100 diluted in water) served as a template for complementary DNA (cDNA) synthesis using RevertAid reverse transcriptase (Thermo Fisher Scientific, EP0442) and random hexamer primers. RT-qPCR was performed on a QuantStudio 5 (Applied Biosystems) using Luna Universal qPCR Master Mix (NEB, M3003E) with 2.5 μ l of 1:20 diluted cDNA as the template in 5- μ l reactions. The cycling conditions were 95 $^{\circ}\text{C}$ for 60 s, followed by 45 cycles of 95 $^{\circ}\text{C}$ for 15 s and 60 $^{\circ}\text{C}$ for 30 s. Relative transcript abundance was first normalized to the respective controls (HEK293FT cells transduced or transfected with inactive *RfxCas13d*) and then to the spike-in ERCC096 using the $\Delta\Delta C_t$ method. By using the ERCC spike-in normalization instead of endogenous gene normalization (for example, *GAPDH* or *ACTB*), we were able to detect global shifts in RNA abundance if present. ERCC130 served as an internal control for computing and comparing gene expression across conditions. For RT-qPCR in Supplementary Figs. 5 and 7, 500 ng of total RNA was used as the template for cDNA synthesis and RT-qPCR was performed using the same conditions as described above. Transcript abundance was normalized to *ACTB* and NT control gRNAs using the $\Delta\Delta C_t$ method. Primer sequences are provided in Supplementary Table 6.

Pooled Cas13 libraries: design and cloning

In total, we performed three pooled Cas13 screens (screen 1: nonessential and essential genes; screen 2: *HDAC1* and *HDAC2* paired titration; screen 3: high-fidelity Cas13 screen) and the design and cloning of each library is described below.

For screen 1, we designed an *RfxCas13d* gRNA library targeting 4,177 human protein-coding gene transcripts. The genes were categorized into three different groups of essentiality on the basis of all CRISPR-Cas9 screens from Hart et al.¹⁴ with 3,448 genes being

nonessential (DepMap release 05-2023; $-0.25 \leq \text{DepMap score} \leq 0.5$), 488 selectively essential ($-1 \leq \text{DepMap score} < -0.25$) and 241 essential (DepMap score < -1). To rationally identify a relationship between target gene expression and collateral RNA degradation, we chose genes over a large range of gene expression values (spanning <1 to $>1,000$ TPM).

For this pooled screen, we designed optimized gRNAs using a model for Cas13 gRNA design trained on thousands of gRNAs (<http://cas13design.nygenome.org>)¹¹. For each transcript, we selected four gRNAs from the highest (or second highest as needed) efficacy quartile (as given by cas13design). We also embedded 1,000 NT gRNAs as negative controls, which we ensured had three or more mismatches to any other transcripts (GENCODE v19, hg19). In total, the library included 17,708 gRNAs. Each gRNA was flanked with constant regions (for PCR amplification and Gibson cloning) and synthesized as 106-mer single-stranded oligonucleotides (Twist Biosciences). A full list of gRNA sequences for the screen 1 library can be found in Supplementary Table 1.

For screen 2 (*HDAC1* and *HDAC2* synthetic lethality titration screen), we first selected 20 pairs of target sites for each gene. For each target site (in *HDAC1* or *HDAC2*), we designed one perfect-match gRNA (that is, the target site itself) and ten additional single-mismatch variant gRNAs with titrated transcript knockdown activities ranging from 5% to 95% (incrementing at every decile) that were designed using the TIGER model library¹³. Each target site in *HDAC1* was paired with each target site in *HDAC2* in a dual gRNA array. For each target site pair, we used 11 *HDAC1* titration gRNAs \times 11 *HDAC2* titration gRNAs \times 2 positions (*HDAC1*–*HDAC2* gRNA order or *HDAC2*–*HDAC1* gRNA order), which yielded 242 combinations for each target site pair. Given the 20 pairs of target sites, we generated a total of 4,839 *HDAC1/HDAC2* arrays. We also paired each gRNA targeting *HDAC1* or *HDAC2* with a NT gRNA. This yielded an additional 880 arrays (11 gRNAs per target site \times 40 total target sites (20 in *HDAC1*, 20 in *HDAC2*) \times 2 positions (*HDAC1/2*–NT gRNA order or NT–*HDAC1/2* gRNA order). We also included 492 arrays with NT gRNAs in both positions. In total, the library for screen 2 consisted of 6,211 arrays. Each gRNA was flanked with constant regions (for PCR amplification and Gibson cloning) and synthesized as 148-mer single-stranded oligonucleotides (Twist Biosciences). A full list of gRNA sequences for the screen 2 library can be found in Supplementary Table 3.

For screen 3 (hfCas13d screen), we screened a gRNA library that was previously used to train the TIGER deep learning model¹³. Briefly, the library contained gRNAs targeting 4,890 genes of varying degrees of essentiality as follows: 785 highly essential genes (DepMap release 05-2023; DepMap score < -1 in $\geq 1,000$ cell lines), 1,537 selective genes ($-1 \leq \text{DepMap score} < -0.25$) and 2,568 nonessential genes (DepMap score ≥ -0.25), all spanning a wide range of gene expression values from 1 to $>1,000$ TPM. For all 4,890 target genes, we designed eight gRNAs targeting the genes protein-coding region. We added 998 NT control gRNAs with more than three mismatches to the hg19 transcriptome. In total, the library consisted of 40,118 gRNAs. Each gRNA was flanked with constant regions (for PCR amplification and Gibson cloning) and synthesized as 106-mer single-stranded oligonucleotides (Twist Biosciences). A full list of gRNA sequences for the screen 3 library can be found in Supplementary Table 4.

For library cloning, CRISPR RNA (crRNA) libraries were amplified using eight replicate 50- μ l PCR reactions with eight amplification cycles. Following gel purification, the resulting amplicon was Gibson-cloned into BsmBI-digested pLentiRNAGuide_003 (Addgene, 138151). We verified successful cloning by Illumina sequencing to verify high gRNA recovery ($>99\%$) and minimal bias (90:10 ratio < 5).

Pooled lentiviral production

Lentivirus was produced by transfection of pooled library plasmids with appropriate packaging plasmids (psPAX2, Addgene, 12260;

pMD2.G, Addgene, 12259) using linear PEI (MW = 25,000; Polysciences, 23966) in HEK293FT. Cells were seeded at 10 million per 10-cm dish and transfected with 60 μ l of PEI, 9.2 μ g of lentiviral gRNA transfer plasmid pool (pLentiRNAGuide_003), 6.4 μ g of psPAX2 and 4.4 μ g of pMD2.G. Then, 3 days after transfection, the viral supernatant was collected and filtered through a 0.45- μ m filter and then stored at -80°C until further use. To minimize the introduction of multiple gRNAs per cell, the lentivirus volume used for transduction was titrated to result in 30–40% survival after puromycin selection.

Pooled Cas13 library CRISPR screens

Cas13d-expressing cells were transduced with the pooled library lentivirus, ensuring at least a 1,000 \times guide representation in the pool of cells per separate infection replicate. They were transduced by spinfection at 1,000 rpm for 1 h at 30°C (Beckman Coulter, Allegra X-14R), followed by overnight incubation. After 24 h, the medium was changed and supplemented with $1 \mu\text{g ml}^{-1}$ puromycin (Thermo Fisher Scientific, A1113803) added. Puromycin selection was completed within 48 h for all cell lines.

Following puromycin selection, Cas13d expression was induced by replenishing with growth medium containing $1 \mu\text{g ml}^{-1}$ puromycin, $5 \mu\text{g ml}^{-1}$ blasticidin and $1 \mu\text{g ml}^{-1}$ doxycycline. Cells were passaged every 2–4 days and split as needed. Samples were harvested at 0, 7 and 14 days after Cas13d induction. Genomic DNA was isolated from cell pellets with a representation of at least 1,000 cells per construct using the following protocol¹⁸: for 100 million cells, 12 ml of NK lysis buffer (50 mM Tris, 50 mM EDTA and 1% SDS, pH 8) was used to lyse cell pellets. Then, 60 μ l of 20 mg ml^{-1} proteinase K (Qiagen) was added to resuspended cells and incubated at 55°C overnight. The next day, 60 μ l of 20 mg ml^{-1} RNase A (Qiagen) was added to cells and incubated at 37°C for 30 min. After, 4 ml of prechilled 7.5 M ammonium acetate was added and samples were vortexed and spun at 4,000g for 10 min. The supernatant was moved to a new tube and mixed well with 12 ml of isopropanol before being spun at 4,000g for 10 min. DNA pellets were washed with 12 ml of 70% ethanol and then spun down. After ethanol removal, pellets were dried and then resuspended with 0.2 \times TE buffer (Sigma-Aldrich).

We amplified gRNA cassettes from the genomic DNA using a two-step PCR protocol (PCR1 and PCR2). PCR1 was performed to amplify a region containing the gRNA cassette in the lentiviral genomic integrant using TaqB polymerase (Enzymatics, P7250L). We performed an appropriate number of PCR1 reactions for each gDNA sample on the basis of library size (screen 1, 40 reactions; screen 2, 20 reactions; screen 3, 48 reactions) using 10 μ g of gDNA per 100- μ l PCR1 reaction (teb cycles). We then combined PCR1 products for the same sample together before PCR2, which was performed to incorporate Illumina adaptors using Q5 polymerase (NEB, M0491). We performed an appropriate number of PCR2 reactions for each sample (screen 1, 16 reactions; screen 2, 8 reactions; screen 3, 24 reactions) using 5 μ l of unpurified PCR1 product per 50- μ l reaction (18 cycles). The resulting amplicons from PCR2 (~ 270 bp) were pooled and then purified using SPRI beads (Beckman, B23317) or gel extracted using a QiaQuick gel extraction kit (Qiagen, 28704). The concentration of the purified PCR product was quantified using Qubit double-stranded DNA HS assay kit (Thermo Fisher Scientific, Q32851) and sequenced on an Illumina NextSeq 500 using a single-ended 150-cycle read.

Pooled screen analysis

We processed reads from pooled Cas13d screens following established pipelines⁴: First, reads were demultiplexed on the basis of Illumina i7 barcodes present in PCR2 reverse primers and custom in-read i5 barcodes, allowing for one mismatch. Reads were trimmed to the expected gRNA length by identifying known anchor sequences relative to the guide sequence. Reads were

trimmed using Cutadapt (version 1.13)¹⁹ with the following parameters: -g CTGGTCCGGGTTTGAAC -e 0.2 -O 5 --discard-untrimmed and -a TTTTGAATTCGCTAGCT -e 0.1 -O 5 --minimum-length 15 --discard-untrimmed.

We aligned processed reads to the designed gRNA reference using Bowtie (version 1.1.2)²⁰ and allowed for up to three mismatches (parameters: -v 1 -m 3 --best -q) for screen 1 and screen 3. For screen 2 (*HDAC1* and *HDAC2* titration), processed reads were collapsed (FASTX-Toolkit) to count perfect duplicates followed by exact string-match intersection with the reference such that only perfectly matching and unique alignments were kept. The raw gRNA counts were normalized using a median of ratio method²¹ and batch-corrected for biological replicates using combat from the SVA R package (version 3.34.0)²². Nonreproducible technical outliers were removed by pairwise linear regression for each sample, collecting residuals and taking the median value for individual gRNAs across each time point.

To calculate gRNA depletion, count ratios between the late time point (day 14) and the early time point (day 0) sample for each replicate were computed followed by \log_2 transformations. Consistency across replicates was assessed using Pearson correlations. We quantified the mean \log_2 fold change using all gRNAs targeting each gene and calculated the significance of a gene's depletion using robust rank aggregation²³ (RobustRankAggreg version 1.1). For screen 2 (*HDAC1/2* titration), which contains gRNAs with mismatches, we computed the ratio of the fold change of the permuted gRNA to the fold change of the perfect-match reference gRNA¹³; these computations were performed in log space.

RNA immunoprecipitation (RIP)

For the RIP experiments related to screen 2, we transduced A375 wild-type cells with a lentivirus containing a nuclease-inactive *RfxCas13d* (pooled screen nomenclature described above). For screen 3 RIP experiments, we transduced HAP1 cells with lentiviruses containing inactive *RfxCas13d* or inactive *hfCas13d*. We performed lentiviral transduction at a low MOI (<0.3) and selected cells with $5 \mu\text{g ml}^{-1}$ blasticidin S. We then transduced these cells with lentiviruses containing gRNAs (pLentiRNAguide_004). Cells were selected for 72 h using $1 \mu\text{g ml}^{-1}$ puromycin and then induced with doxycycline ($1 \mu\text{g ml}^{-1}$) for an additional 72 h. After that, 1×10^7 cells were collected, washed with $1 \times$ DPBS and lysed with 1 ml of RIP buffer (50 mM Tris-HCl buffer pH 7.5 (Thermo Fisher Scientific, 15567027), 100 mM sodium chloride (Sigma, S5150), 1% NP-40 (Thermo Fisher Scientific, 85124), 0.1% SDS (Sigma, L3771) and 0.5% sodium deoxycholate (Sigma, D6750)). Immediately before using, we added 5 μl of benzonase (Millipore-Sigma, 70746-4) per 1 ml of RIP buffer. Using the RIP buffer supplemented with benzonase, we then performed lysis for 15 min at room temperature.

For input controls, 20 μl of lysate was set aside for western blotting and 80 μl of lysate was used for RNA isolation (input). The remaining lysate was incubated with 30 μl of anti-HA magnetic beads (Sigma, SAE0197) for 2 h at 4 °C. After three washes with 1 ml of RIP buffer, the beads were resuspended in 100 μl of RIP buffer. Of this, 20 μl was used for western blotting and 80 μl was used for RNA isolation (Cas13 pulldown enrichment). Protein-RNA complexes were denatured in NuPAGE LDS sample buffer supplemented with 100 mM DTT for 10 min at 65 °C. Protein enrichment compared to input samples was analyzed by western blotting, as described above.

Copurified RNAs were isolated using the Direct-zol RNA purification kit and used as templates for cDNA synthesis using RevertAid reverse transcriptase and random hexamer primers. RNA enrichment in immunoprecipitation samples was measured by RT-qPCR. RT-qPCR was performed on a QuantStudio 5 using Luna Universal qPCR master mix with 2.5 μl of 1:20 diluted cDNA as the template in 5- μl reactions. The cycling conditions were 95 °C for 60 s, followed by 45 cycles of 95 °C for 15 s and 60 °C for 30 s. The mRNA enrichment

for targeting gRNAs was calculated in immunoprecipitation samples by first normalizing for cell number (using the matched input sample) and then for target enrichment (using cells transduced with NT control gRNAs).

Reporting summary

Further information on research design is available in the Nature Portfolio Reporting Summary linked to this article.

Data availability

All data generated in this study can be downloaded from the National Center for Biotechnology Information under accession number PRJNA1177779. This study also uses HEK293FT and HAP1 RNA-sequencing data (PRJNA1161603) and DepMap Consortium data (23Q2: https://depmap.org/portal/data_page/).

References

- Chen, S. et al. Genome-wide CRISPR screen in a mouse model of tumor growth and metastasis. *Cell* **160**, 1246–1260 (2015).
- Martin, M. Cutadapt removes adapter sequences from high-throughput sequencing reads. *EMBnet J.* **17**, 10–12 (2011).
- Langmead, B., Trapnell, C., Pop, M. & Salzberg, S. L. Ultrafast and memory-efficient alignment of short DNA sequences to the human genome. *Genome Biol.* **10**, R25 (2009).
- Love, M. I., Huber, W. & Anders, S. Moderated estimation of fold change and dispersion for RNA-seq data with DESeq2. *Genome Biol.* **15**, 550 (2014).
- Leek, J. T., Johnson, W. E., Parker, H. S., Jaffe, A. E. & Storey, J. D. The sva package for removing batch effects and other unwanted variation in high-throughput experiments. *Bioinformatics* **28**, 882–883 (2012).
- Kolde, R., Laur, S., Adler, P. & Vilo, J. Robust rank aggregation for gene list integration and meta-analysis. *Bioinformatics* **28**, 573–580 (2012).

Acknowledgements

We thank the entire N.E.S. laboratory for support and advice. We thank the New York University Biology Genomics Core for sequencing resources. N.E.S. acknowledges support from the National Institutes of Health (NIH) National Human Genome Research Institute (DP2HG010099 and R01HG012790), NIH National Cancer Institute (R01CA218668 and R01CA279135), NIH National Institute of Allergy and Infectious Diseases (R01AI176601), NIH National Heart, Lung and Blood Institute (R01HL168247), National Science Foundation (EAGER 2409037), Simons Foundation for Autism Research (Genomics of ASD 896724), Chan-Zuckerberg Initiative, MacMillan Center for the Study of the Noncoding Cancer Genome, New York University and New York Genome Center.

Author contributions

S.K.H. and N.E.S. conceptualized the project. H-H.W. and N.E.S. designed the Cas13 libraries. S.K.H., H-H.W. and A.M-M. performed pooled Cas13 screens. S.K.H., H-H.W. and S.M. analyzed pooled screens. S.K.H., S.M., G.D. and O.C. conducted validation assays. N.E.S. supervised the work. S.K.H., S.M. and N.E.S. wrote the manuscript with input from all authors.

Competing interests

H-H.W. is a cofounder of Neptune Bio. N.E.S. is an adviser to Qiagen and a cofounder and adviser of TruEdit Bio and OverT Bio. The remaining authors declare no competing interests.

Additional information

Supplementary information The online version contains supplementary material available at <https://doi.org/10.1038/s41587-025-02558-3>.

Correspondence and requests for materials should be addressed to Neville E. Sanjana.

Peer review information *Nature Biotechnology* thanks Claes Wahlestedt, Amit Deshwar and the other, anonymous, reviewer(s) for their contribution to the peer review of this work.

Reprints and permissions information is available at www.nature.com/reprints.

Reporting Summary

Nature Portfolio wishes to improve the reproducibility of the work that we publish. This form provides structure for consistency and transparency in reporting. For further information on Nature Portfolio policies, see our [Editorial Policies](#) and the [Editorial Policy Checklist](#).

Statistics

For all statistical analyses, confirm that the following items are present in the figure legend, table legend, main text, or Methods section.

n/a | Confirmed

- The exact sample size (n) for each experimental group/condition, given as a discrete number and unit of measurement
- A statement on whether measurements were taken from distinct samples or whether the same sample was measured repeatedly
- The statistical test(s) used AND whether they are one- or two-sided
Only common tests should be described solely by name; describe more complex techniques in the Methods section.
- A description of all covariates tested
- A description of any assumptions or corrections, such as tests of normality and adjustment for multiple comparisons
- A full description of the statistical parameters including central tendency (e.g. means) or other basic estimates (e.g. regression coefficient) AND variation (e.g. standard deviation) or associated estimates of uncertainty (e.g. confidence intervals)
- For null hypothesis testing, the test statistic (e.g. F , t , r) with confidence intervals, effect sizes, degrees of freedom and P value noted
Give P values as exact values whenever suitable.
- For Bayesian analysis, information on the choice of priors and Markov chain Monte Carlo settings
- For hierarchical and complex designs, identification of the appropriate level for tests and full reporting of outcomes
- Estimates of effect sizes (e.g. Cohen's d , Pearson's r), indicating how they were calculated

Our web collection on [statistics for biologists](#) contains articles on many of the points above.

Software and code

Policy information about [availability of computer code](#)

Data collection

Pooled screen data pre-processing: Sequencing reads were trimmed using Cutadapt (v.1.13) and processed reads were aligned using bowtie (v.1.1.2) with up to 3 mismatches allowed. For the HDAC1/HDAC2 titration screen, read counts were processed using FASTX-Toolkit (v0.0.14) Flow cytometry data was collected with SH800S Cell Sorter Software (v 2.1.5) Imaging data was collected with Incucyte S3 v2023A (Sartorius) or BZ-X810 Keyence.

Data analysis

Pooled screen data processing:
R (v4.2.3)
RobustRankAggreg (v1.1)
SVA (v3.34.0)

Flow cytometry data was analyzed with FlowJo (version 10.10.0)
Imaging data was analyzed using Incucyte Live Cell Analysis or Keyence BZ-H4C Hybrid Cell Count software.

For manuscripts utilizing custom algorithms or software that are central to the research but not yet described in published literature, software must be made available to editors and reviewers. We strongly encourage code deposition in a community repository (e.g. GitHub). See the Nature Portfolio [guidelines for submitting code & software](#) for further information.

Data

Policy information about [availability of data](#)

All manuscripts must include a [data availability statement](#). This statement should provide the following information, where applicable:

- Accession codes, unique identifiers, or web links for publicly available datasets
- A description of any restrictions on data availability
- For clinical datasets or third party data, please ensure that the statement adheres to our [policy](#)

All data generated in this study are available from BioProject PRJNA1177779. HEK293FT and HAP1 RNA-sequencing data is from BioProject PRJNA116160. The publicly available DepMap Consortium dataset was also used in this study (23Q2: https://depmap.org/portal/data_page/).

Research involving human participants, their data, or biological material

Policy information about studies with [human participants or human data](#). See also policy information about [sex, gender \(identity/presentation\), and sexual orientation](#) and [race, ethnicity and racism](#).

Reporting on sex and gender	N/A
Reporting on race, ethnicity, or other socially relevant groupings	N/A
Population characteristics	N/A
Recruitment	N/A
Ethics oversight	N/A

Note that full information on the approval of the study protocol must also be provided in the manuscript.

Field-specific reporting

Please select the one below that is the best fit for your research. If you are not sure, read the appropriate sections before making your selection.

Life sciences Behavioural & social sciences Ecological, evolutionary & environmental sciences

For a reference copy of the document with all sections, see [nature.com/documents/nr-reporting-summary-flat.pdf](https://www.nature.com/documents/nr-reporting-summary-flat.pdf)

Life sciences study design

All studies must disclose on these points even when the disclosure is negative.

Sample size	No sample size calculations were performed.
Data exclusions	No experimental replicates were excluded.
Replication	All pooled screens have been conducted with at least two replicate experiments and replicates were conducted independently. All validation experiments were conducted with at least two replicates and orthogonal experiments to ensure robustness of the phenotype. All attempts at replication were successful.
Randomization	Randomization was not performed as we used no subjective quantification.
Blinding	Not applicable. Blinding is not relevant to our study because it is not a subjective trial and the results presented here are purely based on objective description of our experiments.

Reporting for specific materials, systems and methods

We require information from authors about some types of materials, experimental systems and methods used in many studies. Here, indicate whether each material, system or method listed is relevant to your study. If you are not sure if a list item applies to your research, read the appropriate section before selecting a response.

Materials & experimental systems

Methods

n/a	Involved in the study
<input type="checkbox"/>	<input checked="" type="checkbox"/> Antibodies
<input type="checkbox"/>	<input checked="" type="checkbox"/> Eukaryotic cell lines
<input checked="" type="checkbox"/>	<input type="checkbox"/> Palaeontology and archaeology
<input checked="" type="checkbox"/>	<input type="checkbox"/> Animals and other organisms
<input checked="" type="checkbox"/>	<input type="checkbox"/> Clinical data
<input checked="" type="checkbox"/>	<input type="checkbox"/> Dual use research of concern
<input checked="" type="checkbox"/>	<input type="checkbox"/> Plants

n/a	Involved in the study
<input checked="" type="checkbox"/>	<input type="checkbox"/> ChIP-seq
<input type="checkbox"/>	<input checked="" type="checkbox"/> Flow cytometry
<input checked="" type="checkbox"/>	<input type="checkbox"/> MRI-based neuroimaging

Antibodies

Antibodies used

anti-HA Cell Signaling Technology 2367S
 anti-HDAC1 Proteintech 10197-1-AP
 anti-beta-tubulin Invitrogen 32-2600
 donkey anti-mouse IRDye 800CW LI-COR 925-32212

anti-CD46 BioLegend 352405 clone TRA-2-10
 anti-CD55 BioLegend 311306 clone JS11

Validation

HA-tag- From manufacturer's website: HA-Tag (6E2) Mouse mAb detects recombinant proteins containing the HA epitope tag. The antibody recognizes the HA-tag fused to either the amino or carboxy terminus of targeted proteins in transfected cells. Species Reactivity: All species expected.

HDAC1 Polyclonal antibody- From manufacturer's website: 10197-1-AP targets HDAC1 in WB, IHC, IF/ICC, IP, CoIP, ChIP, ELISA applications and shows reactivity with human, mouse, rat samples.

Beta Tubulin Monoclonal Antibody- From manufacturer's website: This antibody reacts with the ~50 kDa beta-tubulin and has been shown to bind to the two major and one of the minor beta-tubulin isotypes. Reactivity has been confirmed with mouse NIH3T3 fibroblast cells, rat brain, and mouse testis. Species reactivity: Dog, C. elegans, Human, Mouse, Non-human primate, Rat.

APC anti-human CD46 Antibody- From manufacturer's website: Each lot of this antibody is quality control tested by immunofluorescent staining with flow cytometric analysis. Species reactivity: human.

FITC anti-human CD55 Antibody- From manufacturer's website: Each lot of this antibody is quality control tested by immunofluorescent staining with flow cytometric analysis. Species reactivity: human.

Eukaryotic cell lines

Policy information about [cell lines and Sex and Gender in Research](#)

Cell line source(s)

HEK293FT cells were acquired from Thermo Fisher (R70007). HAP1 cells are from Horizon Discovery (C631). A375 and MDA-MB-231 cells are from ATCC (CRL-1619 and HTB-26).

Authentication

Cell lines were purchased from the manufacturer and not authenticated in the lab.

Mycoplasma contamination

Cell lines were routinely tested for mycoplasma contamination using Lonza MycoAlert (LT07-518) and found to be negative.

Commonly misidentified lines
(See [ICLAC](#) register)

No commonly misidentified cell lines were used.

Plants

Seed stocks

Report on the source of all seed stocks or other plant material used. If applicable, state the seed stock centre and catalogue number. If plant specimens were collected from the field, describe the collection location, date and sampling procedures.

Novel plant genotypes

Describe the methods by which all novel plant genotypes were produced. This includes those generated by transgenic approaches, gene editing, chemical/radiation-based mutagenesis and hybridization. For transgenic lines, describe the transformation method, the number of independent lines analyzed and the generation upon which experiments were performed. For gene-edited lines, describe the editor used, the endogenous sequence targeted for editing, the targeting guide RNA sequence (if applicable) and how the editor was applied.

Authentication

Describe any authentication procedures for each seed stock used or novel genotype generated. Describe any experiments used to assess the effect of a mutation and, where applicable, how potential secondary effects (e.g. second site T-DNA insertions, mosaicism, off-target gene editing) were examined.

Plots

Confirm that:

- The axis labels state the marker and fluorochrome used (e.g. CD4-FITC).
- The axis scales are clearly visible. Include numbers along axes only for bottom left plot of group (a 'group' is an analysis of identical markers).
- All plots are contour plots with outliers or pseudocolor plots.
- A numerical value for number of cells or percentage (with statistics) is provided.

Methodology

Sample preparation

200,000 HAP1 cells per condition were harvested, washed with PBS, and stained with CD46 or CD55 antibody (anti-CD46: BioLegend 352405, clone TRA-2-10, 0.7 μ l per 2×10^5 cells; anti-CD55: BioLegend 311306, clone JS11, 1 μ l per 2×10^5 cells) for 25 minutes on ice. The cells were then washed with PBS 3 times before being resuspended in PBS with DAPI (ThermoFisher L34963, 1 μ M) and acquired on Sony SH800S cell sorter.

Instrument

Sony SH800S

Software

Data acquisition: SH800S Cell Sorter Software version 2.1.5; data analysis: FlowJo version 10.10.0 (BD).

Cell population abundance

100%- all flow cytometry experiments were performed on transduced and fully selected populations.

Gating strategy

Cells were gated by forward and side scatter and signal intensity to remove potential multiplets and additionally gated for living cells using DAPI exclusion (ThermoFisher L34963).

- Tick this box to confirm that a figure exemplifying the gating strategy is provided in the Supplementary Information.